IOP Conf. Series: Materials Science and Engineering **736** (2020) 042013 doi:10.1088/1757-899X/736/4/042013

Hydrogen and carbon monoxide derivation over metal supported on fibrous silica KCC-1

N A A Fatah[1], A A Jalil[1,2*] and K N L K Din[3]

[1]School of Chemical and Energy Engineering, Faculty of Engineering, Universiti Teknologi Malaysia, 81310 UTM Johor Bahru, Johor, Malaysia
[2]Centre of Hydrogen Energy, Institute of Future Energy, Universiti Teknologi Malaysia,81310 UTM Johor Bahru, Johor, Malaysia
[3]Faculty of Science, Universiti Teknologi Malaysia, 81310 UTM Johor Bahru, Johor, Malaysia

*aishahaj@utm.my

Abstract. Methane is the major component of natural gas that greatly contributes to a rise in global concentration of greenhouse gases. The greenhouses gases emission can be significantly reduced by partial oxidation of methane (POM) to the syngas. Additionally, syngas is an important gas material for the production of valuable chemicals and fuels in the industry. In this study, mesoporous silica KCC-1 catalyst was successfully prepared by using microwave assisted hydrothermal technique. Meanwhile, Rh/KCC-1 catalyst was prepared by incipient wetness impregnation method using ($RhCl_3.xH_2O$) as a precursor. Their catalytic activity towards POM reaction was investigated by using fixed bed quartz reactor. Physicochemical properties of both catalysts were characterized with field emission spectroscopy (FESEM), nitrogen physisorption and pyrrole probed infrared spectroscopy. The results obtained suggest that KCC-1 and Rh/KCC-1 exhibited spherical morphology with a high surface area of 812 and 700 m^2/g, respectively. In addition, both catalysts demonstrated a uniform mesopores with the presence of inter and intra-particle porosity. Pyrrole probed IR spectroscopy results showed that Rh/KCC-1 has low concentration of basic sites than KCC-1. The reduction of basic sites concentration gave a better selectivity of syngas product which caused the suppression of side reactions. Rh/KCC-1 exhibited better catalytic activity than KCC-1 with 99.92% conversion of methane and 97.54% selectivity of H_2 at 973 K. It was noteworthy that the addition of Rh significantly increased the rate of methane conversion and selectivity towards main product.

1. Introduction

Methane (CH_4) is the most abundant gas in the atmosphere and always be the major component of natural gas, which consists up to 90% [1]. The combustion of natural gas in chemical plants, refineries, oil wells and landfills releases both CO_2 and unburned CH_4 greenhouse gases [2]. In addition, the concentration of methane has keep rising due to the rapid growth in human activities and naturally created in wetlands [3]. In recent years, dramatic climate change which led to the global warming has become severe due to the increasing amount of greenhouse gases in the atmosphere. The greenhouse gases effect is a natural phenomenon where the nitrous oxide, methane, and carbon dioxide adsorb and emit radiation in the atmosphere. Besides, methane gas is a very powerful greenhouse gas which contributes to the global warming. According to the statistical study, methane traps 25 times more heat in the atmosphere than carbon dioxide (CO_2). Although methane is nontoxic, colourless, odourless and

tasteless, it can also be a dangerous gas which is highly explosive. If the concentration level of the CH_4 in the air mixture reaches 10-15%, explosion may occur [4].

Conversion of methane to syngas (H_2 and CO) is a great importance to improve the environmental air quality by reducing the percentage of methane in the earth's atmosphere. There are diverse sources of the syngas production, for instance, domestic resources, including nuclear, biomass, natural gas, coal and other renewable sources [5]. The production of syngas has received great attention because of their application in chemical industry and ability to replace methane as the fuel and energy supply for the future [1]. Syngas is a valuable gas material in industry for the synthesis of methanol and Fisher-Tropsch synthesis [6]. The high purity hydrogen is utilized as the fuel cells for the generation of electric power [7]. Meanwhile, the carbon monoxide can be used in the acetic acid, ethylene glycol, paints, plastics and pesticides production [8]. Therefore, the utilization of the syngas is significant to the industry and society for everyday life.

Due to the increasing demand for syngas and high purity hydrogen, the chemical reactions which involves the partial oxidation of methane, methane dry reforming and methane steam reforming have attracted the industrial interests [9]. The alternative route for manufacturing syngas from natural gas is partial oxidation of methane (POM). The POM reaction has been intensively investigated for more than 30 years. The catalytic reaction involved the adsorption and activation of methane and chemisorption of oxygen active species on the surface of catalyst. Methane has high molecular stability due to the presence of C-H bonds that are weakly polarized [2]. It is very difficult to activate methane C-H bonds. Relatively, high temperature needs to defeat these drawbacks and at the same time give high yields of product [10]. Hence, the catalyst involved in POM reaction should have a good thermal stability since the catalyst deeply affects the selectivity of H_2 and CO.

Currently, the noble metals with thermally stable support are known to be efficient catalyst for POM reaction. There are many types of noble metal such as Pd, Rh, Ru, Pt and Ir have been investigated thoroughly in POM reaction [9]. All the noble metals showed their own characteristics. Among the other noble metals, Rh has been widely used even though it is the most expensive noble metal because it gives high and stable methane conversion [11]. Rh catalyst has excellent prospects for the industrial application. Meanwhile, Pd catalyst is unsuited for this reaction due to the limited stability of catalyst at high temperature. Nonetheless, the catalyst for POM reaction still needs to be improved based on the performance of the catalyst support. Plus, it was notified that metal deactivation highly depends on the type of support since it is greatly influenced the POM performance [12]. The need of an ideal support material for the active metal is an important requirement for developing the active catalyst.

In recent years, mesoporous fibrous silica KCC-1 catalyst has been used as a catalyst support in fundamental research. It possesses unique spherical morphology surrounded with dendrimeric silica fibers arranged in three dimensions structures to form spheres which give a high surface area [13]. The high surface area allowed high accessibility of the reactant to the active sites of the catalyst [14]. Besides, the silica-based fibrous material has been extensively studied by the researchers due to the good mechanical stability and high hydrothermal stability. Therefore, in this study the unique morphology KCC-1 was used as the support for the Rh metal and its catalytic activity toward POM reaction was investigated. Besides, the physicochemical properties of the catalyst was characterized to relate with the catalytic performance.

2. Experimental

2.1. Synthesis of support material

Fibrous silica (KCC-1) was prepared via modified microemulsion technique equipped with hydrothermal microwave assisted procedure [14]. Firstly, cyclohexane and pentanol were mixed and tetraethoxysilane (TEOS) was added dropwise and labelled as mixture A. Then, mixture B which consisted of urea, cetylpyridinium bromide (CPB) and water were added to the mixture A. Both mixtures were stirred and placed in a Teflon bottle, before being subjected to intermittent microwave

irradiation (5 h). Then, the solid product was centrifuged, oven-dried (110 °C, 12 h) and calcined (550 °C, 6h). The final product was denoted as KCC-1.

2.2. Synthesis of metal loaded fibrous material

The catalyst was prepared via an incipient wetness impregnation method. 0.5 wt% of Rh was loaded onto KCC-1 by dissolving KCC-1 in 10 mL of distilled water and diluted with $RhCl_3.xH_2O$ solution. The resulting solution was mixed under continuous stirring and heated at 80 °C. After impregnation, the catalyst was dried at (110 °C, 12 h) followed by calcinations in air (550 °C, 3h). The sample was denoted as Rh/KCC-1.

2.3. Catalyst characterization

The FESEM-EDX was used to study the structural morphology and the trace amount of the element in the catalysts (JEOL JSM-6701F). Analysis of the textural characteristics was determined using N_2 physisorption (SA3100 Beckman Coulter). FTIR spectroscopy provides information on a specific bond since molecules have specific frequencies of the internal vibration. FTIR analysis were conducted using an Agilent Cary 640 FTIR spectrometer in the mid-IR region (4000-400 cm^{-1}). Pyrrole adsorbed FTIR conducted at ambient temperature was applied to identify the intrinsic basicity of the catalysts.

2.4. Catalytic activity

The performance of the KCC-1 and Rh/KCC-1 was investigated in the fixed-bed quartz reactor in which 0.2 g of catalyst sample was placed in the quartz reactor. Each of the catalyst was pressed into the pellet, crushed, and sieved to the smaller diameter. The quartz wool was used during the reaction to secure the catalyst inside the reactor. The quartz reactor was placed in the high temperature tube furnace and controlled by the K type thermocouple that directly attached to the outer wall of the reactor. The gas mixture consisted of CH_4, O_2, and N_2 were introduced into the system using flow mass controllers. The mixture of methane (200 ml min^{-1}) and oxygen (200 ml min^{-1}) diluted with nitrogen (100 ml min^{-1}) with a total flow rate of 100 ml min^{-1} passed through the catalyst bed. Then, the reactant and gas products were determined using gas chromatograph equipped with the TCD.

3. Results and discussion

3.1. Morphological and textural studies

The morphological properties of KCC-1 and Rh/KCC-1 were analyzed using FESEM and the resulting images are shown in figure 1. KCC-1 demonstrated a uniform spherical structure with well-defined fibrous dendrimeric morphology, which resulted in high accessibility of active sites for the adsorption of methane.

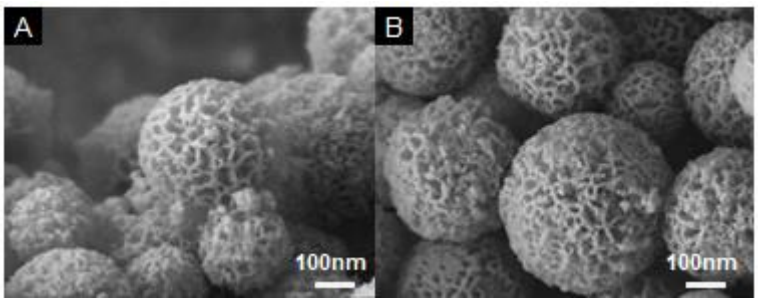

Figure 1. The FESEM images of (A) KCC-1 and (B) Rh/KCC-1.

On the other hand, Rh/KCC-1 possessed similar morphology with the parent KCC-1 despite the addition of noble metal by incipient wetness impregnation. The unique morphology of KCC-1 catalyst remains intact even after incorporation of Rh metal.

Nitrogen physisorption analysis is extensively used to observe the solid porous texture. Figure 2 illustrates the nitrogen physisorption isotherm of KCC-1 and Rh/KCC-1 catalysts. Mesoporous fibrous silica KCC-1 catalyst exhibited a typical type IV isotherms with type H1 hysteresis loops, which indicates a narrow range uniform mesopores with a well define cylindrical-like pore channel [15]. Rh/KCC-1 exhibited almost similar isotherm and similar mesoporous structure with parent KCC-1. Particularly, two steps of capillary condensation were observed for both catalyst at $P/P_\circ = 0.4$ for the first capillary condensation step and $P/P_\circ = 0.9$ for the second capillary condensation step. Both capillary condensation steps determined the intraparticle and interparticle porosity, respectively [15]. Notably, the great difference was observed in capillary condensation at $P/P_\circ = 0.9$ for KCC-1 with respect to Rh/KCC-1. In this step, KCC-1 displayed higher nitrogen uptake which indicated the presence of enormous amount of uniform interparticle pores than noble metal loaded KCC-1 catalysts [16]. The incorporation of noble metal has resulted in the reduction of interparticles porosity due to the metal blockage.

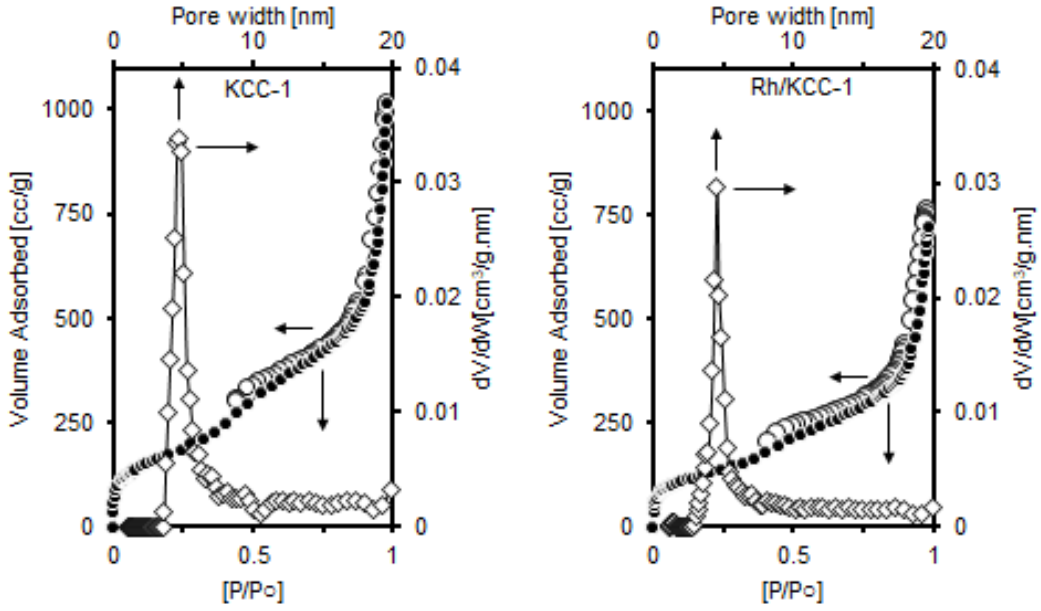

Figure 2. Nitrogen physisorption isotherm and pore size distribution of KCC-1 and Rh/KCC-1.

The non-local density functional theory (NLDFT) method analyzed the pore size distribution of the synthesized catalyst by calculating the specific cumulative surface area over the complete range of micro and meso-pores. The corresponding pore size distribution was displayed in figure 2. Narrow pore size distribution of KCC-1 was observed in the range of 4-6 nm which corresponded to the presence of mesopores from the self-assembly of CTAB surfactant [17]. A formation of smaller pore size of Rh/KCC-1 was observed, probably caused by the deposition of metal on the catalyst surface.

The summarized surface area and pore volume of all catalyst were tabulated in table 1. BET specific surface area of KCC-1 and Rh/KCC-1 catalysts were 812 and 700 m^2/g, respectively. High surface area of KCC-1 could be reasonably attributed to the presence of dendritic fibres [18]. However, the introduction of Rh noble metal to KCC-1 has resulted in the small degradation of specific surface area. It can be observed the surface area of KCC-1 catalyst slightly decreased after the introduction of metals. This phenomenon could be due to the mesopores of the catalyst being blocked

by the deposition of metal particles. The high surface area of KCC-1, promotes high dispersion of Rh metal on the catalyst pore and generate the accessible metal active sites.

Table 1. Textural properties of metal loaded KCC-1.

Catalyst	BET surface area (m^2/g)	Total pore volume (cm^3/g)
KCC-1	812	1.6674
Rh/KCC-1	700	1.4239

3.2. Basicity studies

Infrared spectroscopy with pyrrole probe molecules is commonly used for surface basicity characterizations. The H-donor properties allowed the formation of C_4H_4NH-O bridges with basic oxygen in the framework [19]. Figure 3 illustrates the IR spectra of adsorbed pyrrole on the activated catalysts at different outgassing temperatures. The IR spectra around 3650-3250 cm^{-1} attributed to the N-H stretching vibrations of chemisorbed pyrrole molecules interacting with the basic sites of framework oxygen atoms by hydrogen bonding and interacting simultaneously via the π system with non-framework cation [20]. In particular, the KCC-1 and Rh/KCC-1 catalysts possessed a large shoulder at 3424 cm^{-1} and 3436 cm^{-1}, which can be assigned to the perturbed N-H stretch of pyrrole molecules interacting with the surface of basic sites, respectively [21].

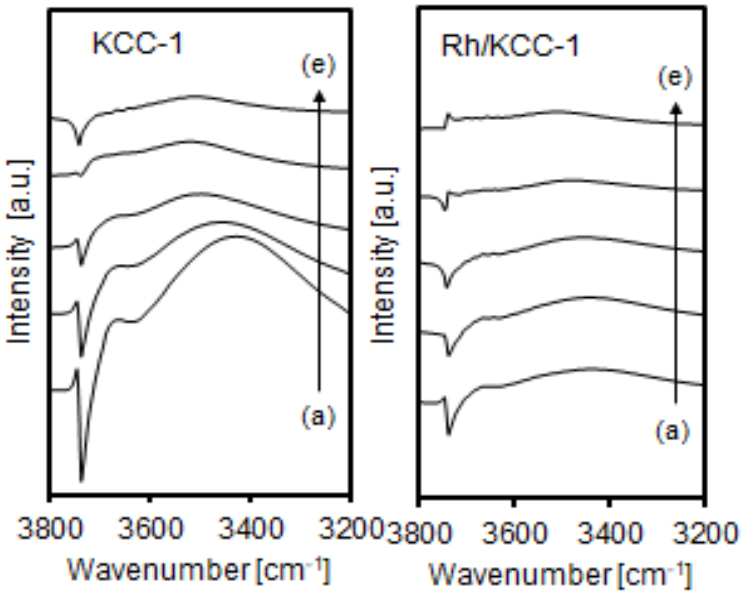

Figure 3. IR spectra of pyrrole adsorbed on KCC-1 and Rh/KCC-1 as a function of outgassing temperature (a) room temperature (b) 50 ºC (c) 100 ºC (d) 150 ºC (e) 200 ºC.

The concentration of basic sites of both catalysts was determined based on their peak intensity. The high peak intensity indicates the high concentration of basic sites possessed by catalyst. It was observed that KCC-1 possessed a higher peak intensity compared to Rh/KCC-1 which can be deduced to the presence of high basic sites concentration on KCC-1. The high concentration of basic sites in KCC-1 was originated from its oxygen vacancy [22]. It can be concluded that the concentration of basic sites was decreased after the incorporation of metal due to the blocking effect of metal which reduced the chemisorption of pyrrole molecules on the catalyst. However, the reduction of basic sites

concentration after rhodium modification could promote the selectivity towards H_2 and suppressed the side reaction. According to the previous study, higher basicity property might lead to the reverse water gas reaction (RWGS) as well as reverse Boudouard reaction [23].

The shifting of IR band around 3650-3250 cm^{-1} assigned to N-H stretching vibration in the gas phase to a lower wavenumber upon the interaction of the H atom in pyrrole with a surface of basic sites could be ascribed to the strength of the basic sites [24]. Strongly bound pyrrole molecules on the catalyst due to the strong hydrogen bond results in high basic sites strength. As shown in figure 3, the KCC-1 peak positioned at lower wavenumber compared to Rh/KCC-1. It was observed the stretching vibration is shifted from 3424 cm^{-1} (KCC-1) to 3436 cm^{-1} (Rh/KCC-1) after the addition of Rh metal. This result clearly indicated the strong interaction of N-H group of pyrrole molecules with the surface basic sites of KCC-1. Therefore, the strength of basic sites decreased upon the introduction of Rh metal.

3.3. Catalytic activity

The catalytic performance of KCC-1 and Rh/KCC-1 catalyst towards partial oxidation of methane to syngas were investigated in a fixed-bed quartz reactor at 600-800 °C using $CH_4/O_2/N_2$ = 4/4/2 as a reaction feed. Figure 4 shows the conversion of CH_4 as a function of the reaction temperature over KCC-1 and Rh/KCC-1. Overall, the methane conversion increased gradually from 600-800 °C and reached up to 99.01% and 99.92% for KCC-1 and Rh/KCC-1, respectively. Both catalysts are active towards POM reaction as both provide a basic site for the dissociation of methane. In addition, the abundance of dendrimer silica fibrous with accessibility of higher active sites also contributed to the high methane conversion.

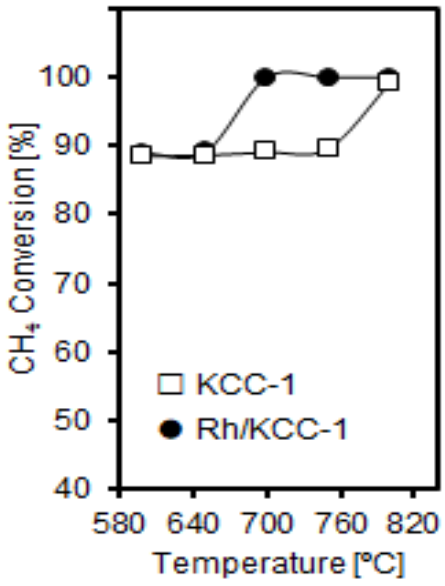

Figure 4. Conversion of CH_4 as a function of the reaction temperature over KCC-1 and Rh/KCC-1.

However, the methane conversion at 700 ºC for KCC-1 and Rh/KCC-1 was obviously differs where the conversion reached 89.04% and 99.89%, respectively. This shows that Rh/KCC-1 is able to convert almost 100% of methane at low temperature. The enhancement in methane conversion at 700 ºC for Rh/KCC-1 catalyst was due to the presence of metal active sites which required for the adsorption and dissociation of methane [25]. Rh/KCC-1 presented a good thermal stability as it able to

promote the rate of desired reaction at low temperature. Therefore, the unmodified support catalyst was presumed to have a poor catalytic activity towards partial oxidation of methane in which the results gave only 89.04% conversion of CH_4 with 70.42% selectivity for H_2 at 700 °C.

Figure 5 represents products selectivity in POM reaction for both catalysts. Notably, no hydrogen formation was observed at low temperature as both catalysts are selective towards side product. However, as the temperature reached 700 °C, the selectivity towards H_2 gradually increased. Excellent performance of POM reaction with better selectivity was observed over Rh/KCC-1. Rh/KCC-1 acquires very significant H_2 selectivity at 700 °C compared to KCC-1 which gave 96.50% and 70.42%, respectively. In POM reaction, the presence of basic sites was significant as the methane conversion increased by increasing the concentration of basic sites. Even so, the excess amount of basic sites concentration in KCC-1 may enhance the selectivity towards CO_2 and suppressed the H_2 and CO selectivity. As shown in table 2, selectivity of CO_2 over Rh/KCC-1 is lower than KCC-1. It can be deduced to the presence of low basic sites in KCC-1 which greatly contributed to the suppression of CO_2 during POM reaction and produced syngas (H_2 and CO) as the main products [26]. Hence, the material with low basicity serve as a good active sites which required for better performance of POM reaction.

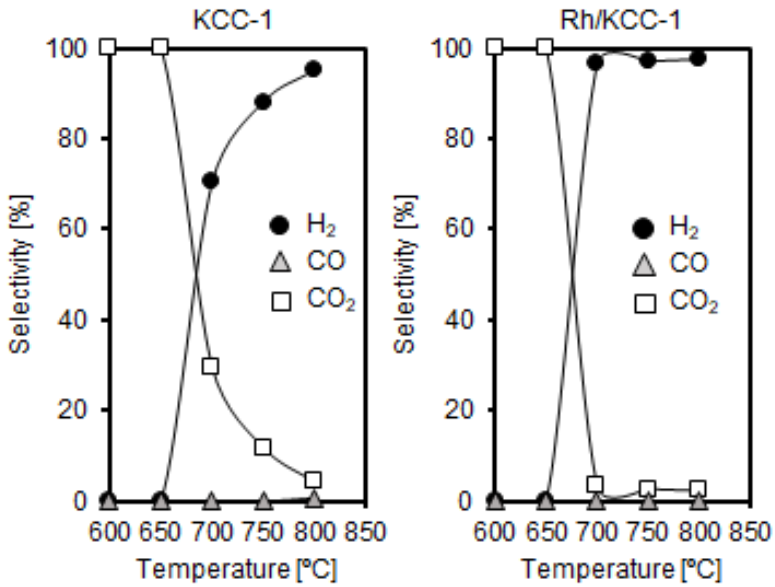

Figure 5. Selectivity of products over KCC-1 based catalysts.

The yield of products for both catalysts is tabulated in table 2. At temperatures lower than 700 °C, no H_2 was observed and the product was mainly consisted of CO_2. This results clearly indicates the total oxidation of methane are involved in the reaction [6]. The yield towards H_2 increased when the reaction temperature is between 700 ºC - 800 ºC. Rh/KCC-1 showed a sharp increase in H_2 yield from 0% to 96.40%, whereas the H_2 yield of KCC-1 only reached 62.70% at reaction temperature of 700 ºC. Based on these results, it can be deduced that Rh/KCC-1 exhibited better H_2 yield at low temperature. The low H_2 yield of KCC-1 was plausibly attributed to the absence of metal active sites which act as adsorption for the CH_4 [27].

In addition, the nature of support also might influence the product distribution as KCC-1 already exhibited a high number of oxygen vacancy which act as electron deficient species to adsorb and dissociate methane [15]. On the other hand, the strength of basic sites significantly influenced the yield of H_2, CO and CO_2 products. The large number of basic sites could promote the formation of CO_2 and suppressed the H_2 and CO yield. KCC-1 with strong basic sites gave higher CO_2 yield

(26.33%) compared to Rh/KCC-1 (3.29%) at 700 ºC. As tabulated in table 2, the CO yield decreased as the temperature increased. In this reaction, the desorbed CO may re-adsorbed and react with the abundance of active oxygen species in strong basic sites and produced CO_2. Meanwhile, the yield of CO_2 for both catalysts start to decrease at 650 ºC may due to the others reaction mainly methane dry reforming process take place by interacting with remaining methane [28][29].

It is noteworthy that Rh/KCC-1 showed highest activity and selectivity towards POM reaction. This result signified that incorporation of Rh metal significantly enhanced the catalytic activity of catalyst in POM reaction. It can be notified that both catalysts have different activities form one another. Further increasing the reaction temperature, the methane conversion, yield and selectivity of H_2 keep increasing, meanwhile the yield and selectivity of CO and CO_2 keep decreasing for both catalysts.

Table 2. Product yields of methane conversion to syngas over KCC-1 and Rh/KCC-1.

Catalyst	Temperature (ºC)	CH_4 Conversion (%)	Yield [%]		
			H_2	CO	CO_2
KCC-1	600	88.4	0	0	88.4
	650	88.6	0	0	88.6
	700	89.0	62.7	0	26.3
	750	89.5	78.9	0	10.7
	800	99.0	94.7	0.14	4.3
Rh/KCC-1	600	88.9	0	0	88.9
	650	89.0	0	0	89.0
	700	99.9	96.4	0.19	3.3
	750	99.9	97.0	0.18	2.7
	800	99.9	97.5	0.16	2.3

4. Conclusion

Mesoporous fibrous silica KCC-1 and Rh/KCC-1 catalyst with fibrous silica morphology was successfully prepared using the microwave assisted hydrothermal and incipient wetness impregnation method. The catalysts possessed identical spherical morphology with presence of dendrimeric fiber. Based on the nitrogen physisorption analysis, KCC-1 catalyst exhibited mesoporous structure with high surface area of KCC-1 (812 m^2/g) and narrow pore size distribution at 4-6 nm and 20-25 nm. The surface area was slightly decreased after the addition of Rh noble metals onto KCC-1 due to deposition of metal particle on mesopores. Rh/KCC-1 was found to be highly active and selective catalyst towards POM reaction as compared to KCC-1. The catalytic activity over Rh/KCC-1 was observed to be higher than KCC-1 which 99.92 and 99.01%, respectively due to the high dispersion of Rh particles, as well as basic sites in moderate strength. The presence rhodium leads to the formation of active metal sites for the adsorption and dissociation of methane and syngas formation. This phenomenon revealed that the surface containing metallic and basic sites plays an important role in POM reaction. Hence, it can be concluded that Rh/KCC-1 is the promising catalyst towards POM reaction.

Acknowledgement

This work was supported by the Professional Development Research University grant from Universiti Teknologi Malaysia (Grant No.04E07) and Research University Grant from Universiti Teknologi Malaysia (Grant No.19H04).

References

[1] Wang B, Albarracín-Suazo S, Pagán-Torres Y and Nikolla E 2017 *Catal. Today* **285** 147–58
[2] Al-Sayari S A 2013 *Open Catal. J.* **6**
[3] Kamieniak J, Randviir E P and Banks C E 2015 *TrAC Trends Anal. Chem.* **73** 146–57
[4] Shi L, Wang J, Zhang G, Cheng X and Zhao X 2017 *Process Saf. Environ. Prot.* **107** 317–33
[5] Kalamaras C M and Efstathiou A M 2013 *Conf. Pap. Sci., Hindawi*
[6] Au C T and Wang H Y 1997 *J. Catal*. **167** 337–45
[7] Li B, Xu X and Zhang S 2013 *Int. J. Hydrogen Energy* **38** 890–900
[8] Ghoneim S A, El-Salamony R A and El-Temtamy S A 2016 *World J. Eng. Technol.* **4** 116
[9] Tsang S C, Claridge J B and Green M L H 1995 *Catal. Today* **23** 3–15
[10] Wang H, Schmack R, Paul B, Albrecht M, Sokolov S and Rümmler S 2017 *Appl. Catal. A Gen.* **537** 33–9
[11] Yan Q G, Wu T H, Weng W Z, Toghiani H, Toghiani R K and Wan H L 2004. *J. Catal*. **226** 247–59
[12] Gronchi P, Centola P and Del Rosso R 1997 *Appl. Catal. A Gen.* **152** 83–92
[13] Polshettiwar V, Cha D, Zhang X and Basset J M 2010 *Angew. Chemie - Int Ed* **49** 9652–6
[14] Fatah N A A, Triwahyono S, Jalil A A, Salamun N, Mamat C R and Majid Z A 2017 *Chem. Eng. J.* **314** 650–9
[15] Hamid M Y S, Firmansyah M L, Triwahyono S, Jalil A A, Mukti R R, Febriyanti E, Suendo V, Setiabudi H D, Mohamed M and Nabgan W 2017 *Appl. Catal. A Gen.* **532** 86–94
[16] Teh L P, Triwahyono S, Jalil A A, Firmansyah M L, Mamat C R and Majid Z A 2016 *Appl. Catal. A. Gen.* **523** 200–8
[17] Ghani N N M, Jalil A A, Triwahyono S, Aziz M A A, Rahman A F A, Hamid M Y S, Izan S M and Nawawi M G M 2019 *Chem. Eng. Sci.* **193** 217–29
[18] Kundu P K, Dhiman M, Modak A, Chowdhury A, Polshettiwar V and Maiti D 2016 *Chempluschem* **81** 1142–6
[19] Kučera J, Nachtigall P, Kotrla J, Košová G and Čejka J 2004 *J. Phys. Chem. B* **108** 16012–22
[20] Teh L P, Triwahyono S, Jalil A A, Mukti R R, Aziz M A A and Shishido T 2015 *Chem. Eng. J.* **270** 196–204
[21] Aziz M A A, Jalil A A, Triwahyono S, Mukti R R, Taufiq-Yap Y H and Sazegar M R 2014 *Appl. Catal. B Environ.* **147** 359–68
[22] Hamid M Y S, Firmansyah M L, Triwahyono S, Jalil A A, Mukti R R and Febriyanti E 2017 *Appl. Catal. A Gen.* **532** 86–94
[23] Özdemir H, Faruk Öksüzömer M A and Ali Gürkaynak M 2010 *Int. J. Hydrogen Energy* **35** 12147–60
[24] Forster H, Fuess H, Geidel E, Hunger B, Jobic H and Kirschhock C 1999 *Phys. Chem. Chem. Phys.* **1** 593–603
[25] Ariffin F, Izan S M, Jalil A A, Mamat C R, Basar N and Jaafar J 2017 *Malaysian J. Catal.* **2**
[26] Wu T, Zhu M, Niu Z, Zhong Y, Guan Y and Liu Y 2002 *J. Nat. Gas Chem.* **11** 159–64
[27] Aziz M A A, Jalil A A, Triwahyono S, Mukti R R, Taufiq-Yap Y H, Sazegar M R 2014 A*ppl. Catal. B Environ.* **147** 359–68
[28] Wu T, Yan Q and Wan H 2005 *J. Mol. Catal. A Chem.* **226** 41–8
[29] Mateos-Pedrero C, Carrazan S R G, Blanco R M and Ruiz P 2010 *Catal. Today* **149** 254–9